Materials Research. 2014; 17(4): 920-925
DOI: http://dx.doi.org/10.1590/1516-1439.251813

Synthesis, Characterization and Microwave Dielectric Properties of Flower-like $Co(OH)_2$/C Nanocomposites

Chao Feng[a], Nannan Bi[a], Xianguo Liu[a]*, Chuangui Jin[a], Kai Huang[a],

Feng Xiao[a], Yuping Sun[b] and Siu Wing Or[c]

[a]Anhui Key Laboratory of Metal Materials and Processing, School of Materials Science and Engineering, Anhui University of Technology, 243002, Maanshan, PR China
[b]Center for Engineering Practice and Innovation Education, Anhui University of Technology, 243032, Maanshan, PR China
[c]Department of Electrical Engineering, The Hong Kong Polytechnic University, Hung Hom, Kowloon, Hong Kong

Received: November 12, 2013; Revised: June 18, 2014

Flower-like $Co(OH)_2$/C nanocomposites have been synthesized by a facile hydrothermal method. Flower-like $Co(OH)_2$/C nanocomposites were self-assembled by the nanosheets with the thickness distribution of 50-80 nm and abundant flocculent carbon structures. With the help of transmission electron microscopy and energy dispersive spectrometer, nanosheets were observed to have core/shell structure, in which $Co(OH)_2$ worked as cores and amorphous C as shells. When the as-prepared products were heated for 6 h at 180 °C, the $Co(OH)_2$ cores were amorphous. The heating time increased to 10 h, the $Co(OH)_2$ cores became crystalline. The formation mechanism and the self-assembly evolution process were proposed. The microwave dielectric properties of $Co(OH)_2$/C nanocomposites were investigated in the frequency range of 0.03-18 GHz. Compared with the amorphous $Co(OH)_2$/C nanocomposites, crystalline nanocomposites had the better conductivity.

Keywords: *Nanocomposites, Nanosheets, Core/shell structure, Carbon*

1. Introduction

Nanostructured materials have received much attention because of their novel electronic, optical, magnetic and catalytic properties. In recent decades, much attention has been paid to the core-shell structured nanoparticles, namely 'nanocapsules'[1-5]. Up to now, with the development of local electronic devices, microwave communication, and the rising pollution of electromagnetic (EM) interference, materials with EM-wave absorption in a wide frequency range, with strong absorption, low density, and low cost are more and more desirable. Among these nanocomposites, nanocapsules with magnetic nanoparticles as cores and dielectric shells are of great interest due to the synergetic effect between magnetic and dielectric losses. Recently, the EM-wave absorption properties of non-magnetic material-based nanocomposites have been driving considerable theoretical and experimental investigation. Wang et al synthesized the carbon coated Sn nanorods by arc discharge method and reported that reflection loss (RL) exceeding -20 dB could be realized in any interval within the 2-18 GHz range by choosing an appropriate thickness of the absorbent layer between 1.5 and 9 mm[6]. Zhang et al prepared the carbon-coated Cu nanocapsules and investigated the permittivity in the GHz range[7]. In our previous work, carbon-coated Ti nanocapsules and carbon-coated VC nanocapsules were synthesized by arc discharge method and investigated their EM properties in detail[8,9].

Carbon can be used as EM interference shielding and EM absorption materials, due to their good electrical, low density, thermal stability and excellent mechanical properties. Carbon has been widely used as the outer shell in the nanocapsules as microwave absorbers[10-12]. Compared with nanoparticles without core/shell structure, carbon shell can dramatically improve their EM absorption properties. Recently, transition metal hydrates have attracted great attentions due to their interesting physical and chemical properties. Among them, $Co(OH)_2$ is widely investigated as electrode material, catalytic material and magnetic cooling materia[13-18]. There are few reports on the EM properties of carbon-coated $Co(OH)_2$ nanocomposites.

In this work, we synthesized flower-like $Co(OH)_2$/C composites self-assembled by $Co(OH)_2$/C core/shell structured nanocapsules through a hydrothermal method. The phase composition and microstructure of $Co(OH)_2$/C composites were investigated by means of X-ray diffraction, transmission electron microscopy and energy dispersive spectrometer. The dielectric properties of $Co(OH)_2$/C composites also were investigated in the frequency range of 0.03-18 GHz.

*e-mail: liuxianguohugh@gmail.com

2. Experimental

2.1. *$Co(OH)_2$ nanosheets*

All reagents were analytical grade and used without further purification. The $Co(OH)_2$ nanosheets were synthesized by a hydrothermal method. In a typical process, 0.6g Cobalt-nitrate hexahydrate ($Co(NO_3)_2 \cdot 6H_2O$) was dissolved in 50ml deionized water. The solution turned to be deep green immediately after 2ml ethanol and 20ml diethanolamine were added. The resultant solution was magnetic stirred for 15 min and subsequently transferred into a 100 ml teflon-lined stainless steel autoclave. After heating at 180 °C for 6 h, the tank was naturally cooled down to room temperature. The product was washed by deionized water and ethanol for three times, and finally dried in a vacuum oven at 80 °C for 2 h.

2.2. *Flower-like $Co(OH)_2$/C nanocomposites*

The above black products were dissolved in 100 ml distilled water with 4 g glucose. The mixture was automatically stirred for 15 min and then was transferred into a 150 ml autoclave. The autoclave was sealed and put into a furnace with the temperature of 180 °C. After heating for 6 h, the autoclave was cooled naturally to room temperature. The product was washed with distilled water and ethanol several times to remove impurities before the characterizations. For the preparation of crystalline samples, the heating time increased to 10 h under the same experimental conditions.

2.3. *Material characterization*

The as-prepared sample was characterized by x-ray diffraction equipped with monochromatized Cu-Ka radiation (XRD, Bruker D8) and scanning electron microscopy (SEM, JEOL-6300 F) equipped with energy dispersive spectrometer (EDS) and Transmission electron microscopy (TEM). High-Resolution TEM (HRTEM) images were obtained on a JEOL JEM-2010 TEM. An EDS attached to the TEM was used to analyze the composition of the products. The $Co(OH)_2$/C nanocomposite-paraffin composite was prepared by uniformly mixing $Co(OH)_2$ nanocomposites with paraffin and pressing them into cylinder-shaped compacts. Then the compact was cut into toroidal shape with 7.00 mm outer diameter and 3.04 mm inner diameter. The EM parameters are measured for $Co(OH)_2$/C microsphere-paraffin composite containing 40 wt% $Co(OH)_2$/C, using an Agilent N5244A network analyzer. Coaxial method was used to determine the EM parameters of the toroidal samples in a frequency range of 0.03-18 GHz with a transverse EM mode. The VNA was calibrated for the full two-port measurement of reflection and transmission at each port. The complex permittivity ε_r ($\varepsilon_r = \varepsilon' - \varepsilon''$, where ε' and ε'' are the real and imaginary parts of ε_r, respectively) was calculated from S-parameters tested by the VNA, using the simulation program of Reflection/ Transmission Nicolson–Ross model[18].

3. Results and Discussion

Figure 1 shows the XRD patterns of products with heating time of 6 and 10 h. In Figure 1a, the broad diffraction peak at 20-25° arises from the amorphous carbon. It is worthy noted that there are no peaks for $Co(OH)_2$, indicating that the $Co(OH)_2$ is not crystalline at heating time of 6 h. When the heating time reaches to 10 h, main peaks of $Co(OH)_2$ are observed at 32.48°, 37.90°, 57.92°, 61.52° and 67.94°, corresponding to the reflections of (100), (101), (102), (111) and (200) of $Co(OH)_2$, respectively. All the observed peaks can be matched with the $Co(OH)_2$ (JCPDS no. 34-0443). The average grain size of $Co(OH)_2$ is calculated to be about 30 nm from the full width at half maximum of the $Co(OH)_2$ (101) Bragg scatting peak intensity using Debye-Scherrer's formula $Dm = (0.89\lambda) / [\delta(2\theta)\cos\theta]$, where λ is the X-ray wavelength, $\delta(2\theta)$ is the line broadening at half the maximum intensity in radians, and θ is the Bragg scattering angle.

Figure 2 shows different magnified SEM images of the products with heating time of 6 and 10 h, respectively. All images clearly indicate that the presence of three-dimensional (3D) flower-like structures. As shown in Figure 2a, the as-synthesized $Co(OH)_2$/C sample presents a uniform flower-like microspheres with a averaged diameter of 3 μm. Furthermore, the magnified SEM images (Figure 2b) demonstrate that 3D flower-like microspheres are self-assembled by lots of nanosheets building blocks with the thickness ranging between 40 and 60 nm. In addition, abundant flocculent structures present in the 3D flower-like $Co(OH)_2$/C microspheres, which are amorphous carbon proved by EDS. Figure 2c shows the SEM image of $Co(OH)_2$/C samples with heating time of 10 h. The samples exhibit the uniform flower-like microsphere with a averaged diameter of 4 μm. In Figure 2d, the nanosheets have the thickness ranging between 60 and 80 nm. After being heated for 10 h, the size of microspheres and nanosheets and the amount of flocculent structures evidently increase, since the increasing time is helpful for the growth of microspheres and nanosheets and the decomposition of glucose. It is worthwhile noting that the as-obtained flower-like $Co(OH)_2$/C superstructures cannot be destroyed and broken into the individual $Co(OH)_2$/C nanosheets even after subjecting long-time ultrasonication.

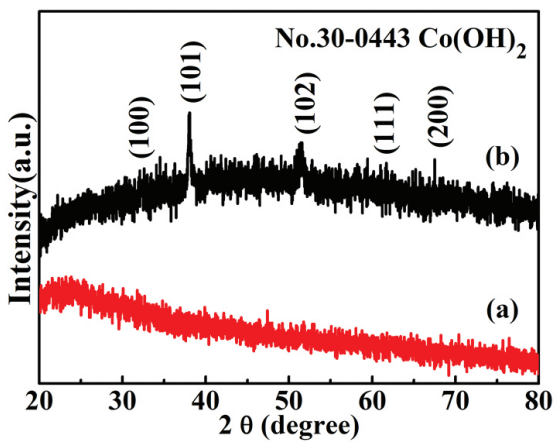

Figure 1. XRD patterns of products with heating time of (a) 6 h and (b) 10 h.

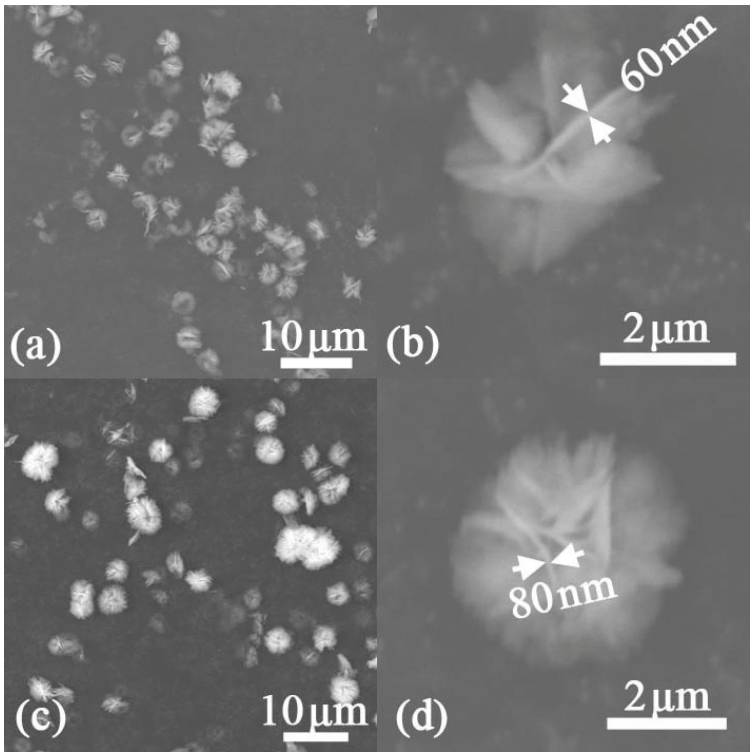

Figure 2. (a) SEM image and (b) magnified SEM image of $Co(OH)_2$/C nanocomposites with heating time of 6 h; (c) SEM image and (d) magnified SEM image of $Co(OH)_2$/C nanocomposites with heating time of 10 h.

Figure 3 presents the formation process of the flower-like $Co(OH)_2$/C nanocomposites. Such a process is consistent with so-called two-steps growth process, which involves a fast nucleation of amorphous primary particles followes by a slow aggregation and crystallization of primary particles[19]. Zhong et al. and Wei et al. have reported similar progress in preparing 3-D flower-like iron oxide and NiCo alloy nanostructures, respectively[20,21]. In our experiment, the process divides into two steps. First, the mixed solution of $Co(NO_3)_2 \cdot 6H_2O$, ethanol, glycolamine and deionized water is heated to 180 °C, and the $Co(OH)_2$ starts to nucleate. The nuclei growth and primary nuclei are formed and the small particle aggregates into plume-like structure nanosheets. Afterwards, the nanosheets assemble into flower-like microspheres. In the process of $Co(OH)_2$/C nanocomposites, the glucose decomposes into carbon particles and H_2O at 180 °C. The small C particles is attached to the surface of the flower-like microspheres, and the $Co(OH)_2$/C nanocomposites are finally formed.

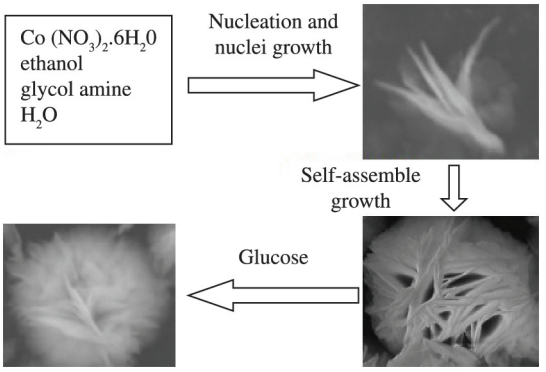

Figure 3. Schematic illustration of the morphology evolution process of the flower-like $Co(OH)_2$/C nanocomposites.

In order to clearly demonstrate their microstructures, the TEM images of 3D flower-like $Co(OH)_2$/C microspheres with different magnifications are shown in Figure 4. Figure 4a clearly shows the amorphous nature of nanosheet structure. Figure 4b demonstrates the element composition of nanosheet structure, in which Cu element is from the Cu grids. As shown in Figure 4c, the clear core-shell structure exists in the present nanosheet structure with heating time of 6 h, in which the amorphous shell has a thickness of 5 nm. The shell material is determined to be carbon from the EDS result (Figure 4d) and the experimental process. Figure 4e exhibits the microstructure of $Co(OH)_2$/C nanocomposites with heating time of 10 h, in which the nanocomposites also have the core-shell structure with a shell of 6 nm. The results are consistent with the SEM results, indicating the heating time has an important influence on the growth and the crystalline of $Co(OH)_2$/C nanocomposites. In addition, the HRTEM image in Figure 4e clearly shows that the d-spacing of 0.24 nm in the core corresponds to the lattice plane {101} of $Co(OH)_2$, indicating $Co(OH)_2$ is crystalline in the nanocomposites with heating tine of 10 h.

As shown in Figure 5, the real part (ε') and imaginary part (ε'') of relative permittivity for the $Co(OH)_2$/C-paraffin composite with 40 wt%. $Co(OH)_2$/C nanocomposites are

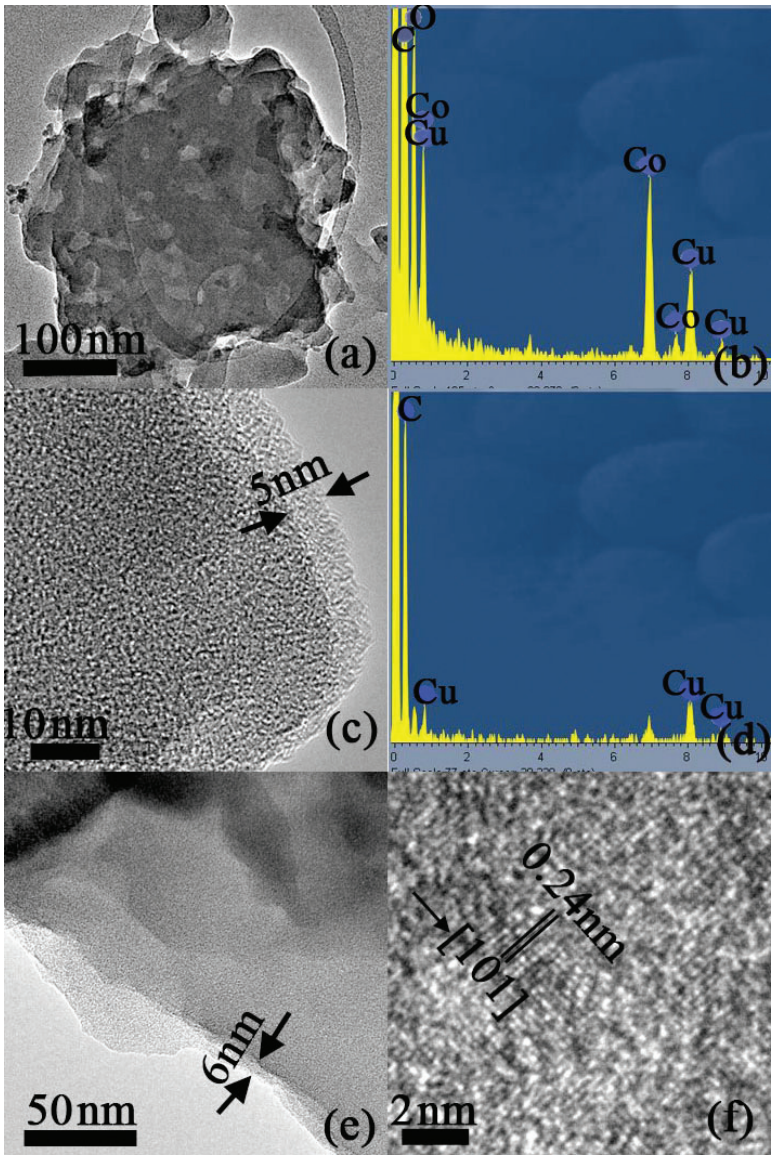

Figure 4. (a) TEM image of $Co(OH)_2$/C nanocomposites with heating time of 6 h, (b) the corresponding EDS pattern, (c) HRTEM image of core-shell structure and (d) the corresponding EDS pattern at the amorphous shell part; (e) TEM image of $Co(OH)_2$/C nanocomposites with heating time of 10 h and (f) the corresponding HRTEM image of the crystalline $Co(OH)_2$ core.

plotted as a function of frequency at 0.03-18 GHz. ε' is relative to the polarization and ε'' implies the dielectric loss in the particles. It can be seen that ε' exhibits the similar variation tendency of decreasing with the frequency increasing from 0.03 to 18 GHz which is due to increased lagging behind of the dipole-polarization response with respect to the electric-field change at higher frequencies[22]. The frequency dependence of ε'' in Figure 5b can be explained by the following equation according to the free electron theory[23] : $\varepsilon'' = \delta / 2\pi\varepsilon_0 f$, where δ is the electrical conductivity, f is frequency and ε_0 is the dielectric constant in vacuum. The conductivity of $Co(OH)_2$/C nanocomposites originates from its free electrons. Except for the natural frequency at around 14 GHz, the ε'' of $Co(OH)_2$/C nanocomposites with heating time of 10 h is higher than that of nanocomposites with heating time of 6 h, indicating that the crystalline state of $Co(OH)_2$ has better conductivity than the amorphous one. As we known, the ideal microwave absorbers with thin layer thickness should process the ability of strong absorption at the broader frequency band. The natural frequency at around 14 GHz indicates the enhanced dielectric loss in a limited frequency range. The dielectric loss is sensitive to the absorbing frequency, which becomes the challenge for high technological applications[24]. In addition, it can be found that ε' and ε'' for $Co(OH)_2$/C nanocomposites exhibit a significant and similar fluctuation, over the 0.03-18 GHz range, ascribed to the displacement current lag at the core/shell interface, similar to the Fe/C and Fe/ZnO nanocapsules[25,26].

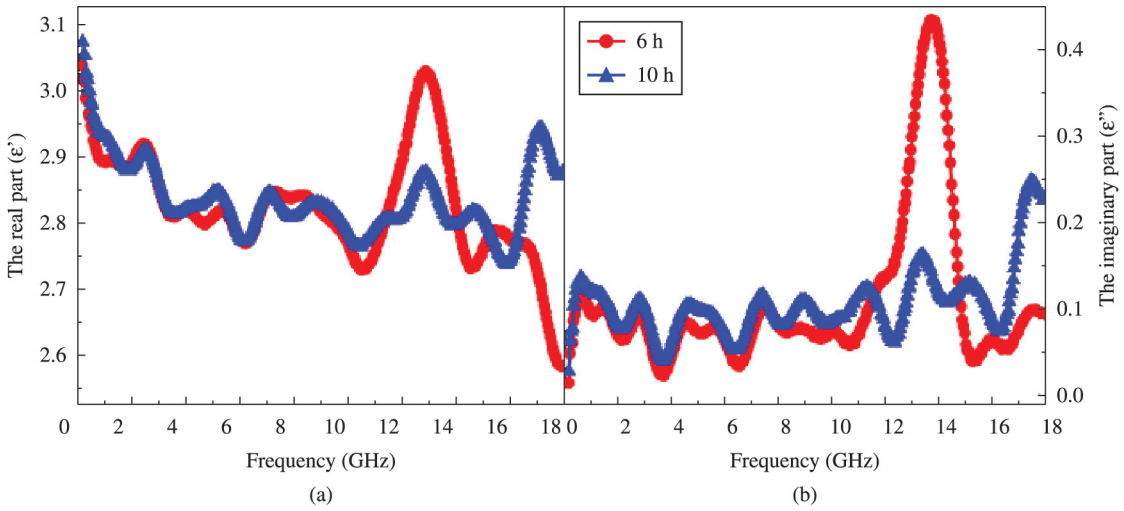

Figure 5. (a) the real part (ε′) and (b) the imaginary part (ε″) of relative complex permittivity for the $Co(OH)_2$/C-paraffin composite at heating time of 6 h and 10 h, respectively.

4. Conclusion

In summary, flower-like $Co(OH)_2$/C nanocomposites were fabricated by a facile hydrothermal method. Flower-like $Co(OH)_2$/C nanocomposites were self-assembled by the nanosheets and abundant flocculent carbon. The size of nanocomposites and amount of flocculent carbon increased with the heating time. TEM results proved the $Co(OH)_2$/C nanocompsoites have core/shell structure, in which $Co(OH)_2$ worked as cores and amorphous carbon as shells. The formation mechanism and the self-assembly evolution process were proposed. The microwave dielectric properties of $Co(OH)_2$/C nanocomposites were investigated in the frequency range of 0.03-18 GHz. Compared with the amorphous $Co(OH)_2$/C nanocomposites, the crystalline nanocomposite had the better conductivity.

Acknowledgements

This study has been supported partly by the National Natural Science Foundation of China (Grant Nos. 51201002), by the Research Grants Council of the HKSAR Government (PolyU 5236/12E), and by The Hong Kong Polytechnic University (G-YK59 and 4-ZZ7L).

References

1. Zhang ZD. Magnetic nanocapsules. *J. Mater. Sci. Technol*. 2007; 23(1):1-25.
2. Liu JR, Itoh M, Horikawa T, Itakura M, Kuwano N and Machida KI. Complex permittivity, permeability and electromagnetic wave-absorption of α-Fe/C (amorphous) and Fe2B/C(amorphous) composites. *J. Phys. D Appl. Phys*. 2004; 37(19):2737-2741. http://dx.doi.org/10.1088/0022-3727/37/19/019
3. Zhang XF, Huang H and Dong XL. Core/shell metal/heterogeneous oxide nanocapsules: the empirical formation law and tunable electromagnetic losses. *J. Phys. Chem. C*. 2013; 117(16):8563-8569. http://dx.doi.org/10.1021/jp4015417
4. Zhang XF, Dong XL, Huang H, Liu YY, Lv B, Lei JP et al. Microstructure and microwave absorption properties of carbon-coated iron nanocapsules. *J. Phys. D Appl. Phys*. 2007; 40(17):5383-5387. http://dx.doi.org/10.1088/0022-3727/40/17/056
5. Yan SJ, Zhen L, Xu CY, Jiang JT and Shao WZ. Microwave absorption properties of FeNi3 submicrometre spheres and SiO2@FeNi3 core-shell structures. *J. Phys. D Appl. Phys*. 2010;43(24). http://dx.doi.org/10.1088/0022-3727/43/24/245003
6. Wang ZH, Han Z, Geng DY and Zhang ZD. Synthesis,characterization and microwave absorption of carbon-coated Sn nanorods. *Chem Phys Lett*. 2010; 489(4-6):187-190. http://dx.doi.org/10.1016/j.cplett.2010.02.056
7. Zhang XF, Dong XL, Huang H, Wang DK, Lv B and Lei JP. High permittivity from defective carbon-coated Cu nanocapsules. *Nanotechnology*. 2007; 18(27). http://dx.doi.org/10.1088/0957-4484/18/27/275701
8. Sun YP, Liu XG, Jin CG, Xia AL, Zhao SS, Li WH et al. A facile route to carbon-coated vanadium carbide nanocapsules as microwave absorbers. *RSC Adv*. 2013; 3:18082-18086. http://dx.doi.org/10.1039/c3ra42544d
9. Liu XG, Geng DY, Jiang JJ, Du J, Yang F, Xie ZG et al. High Dielectric Loss in Graphite-Coated Ti Nanocapsules. *J Nanosci Nanotechnol*. 2010; 10(4):2366-2369. PMid:20355435. http://dx.doi.org/10.1166/jnn.2010.2159
10. Wang T, Han R, Tan GG, Wei JQ, Qiao L and Li FS. Reflection loss mechanism of single layer absorber for flake-shaped carbonyl-iron particle composite. *J Appl Phys*. 2012; 112:104903. http://dx.doi.org/10.1063/1.4767365
11. Yan SJ, Xu CY, Jiang JT, Liu DB, Wang ZY, Tang J et al. Strong dual-frequency electromagnetic absorption in Ku-band of C@FeNi3 core/shell structured microchains with negative permeability. *J Magn Magn Mater*. 2014; 349:159-164. http://dx.doi.org/10.1016/j.jmmm.2013.08.027
12. Zhang XF, Dong XL, Huang H, Liu YY, Wang WN, Zhu XG et al. Microwave absorption properties of the carbon-coated nickel nanocapsules. *Appl Phys Lett*. 2006; 89(5):053115. http://dx.doi.org/10.1063/1.2236965

13. Ko JM, Soundarajan D, Park JH, Yang SD, Kim SW, Kim KM et al. γ-Ray-induced synthesis and electrochemical properties of a mesoporous layer-structured α-Co(OH)2 for supercapacitor applications. *Curr Appl Phys*. 2012; 12(1):341-345. http://dx.doi.org/10.1016/j.cap.2011.07.029

14. Cao L, Xu F, Liang YY and Li HL. Preparation of the novel nanocomposite Co(OH)2/ ultra-stable Y zeolite and its application as a supercapacitor with high energy density. *Adv Mater*. 2004; 16(20):1853-1857. http://dx.doi.org/10.1002/adma.200400183

15. Yao YJ, Xu C, Miao SD, Sun HQ and Wang SB. One-pot hydrothermal synthesis of Co(OH)2 nanoflakes on graphene sheets and their fast catalytic oxidation of phenol in liquid phase. *J Colloid Interface Sci*. 2013; 402:230-236. PMid:23643184. http://dx.doi.org/10.1016/j.jcis.2013.03.070

16. Chen G, Fu EG, Zhou M, Xu Y, Fei L, Deng SG et al. A facile microwave-assisted route to Co(OH)2 and Co3O4 nanosheet for Li-ion battery. *J Alloys Compd*. 2013; 578:349-354. http://dx.doi.org/10.1016/j.jallcom.2013.06.042

17. Ghosh D, Giri S and Das CK. Preparation of CTAB-Assisted Hexagonal Platelet Co(OH)2/Graphene Hybrid Composite as Efficient Supercapacitor Electrode Material. *ACS Sustainable Chem. Eng*. 2013; 1(9):1135-1142. http://dx.doi.org/10.1021/sc400055z

18. Yun YW, Kim SW, Kim GY, Kim YB, Yun YC and Lee KS. Three-dimensional image integration: a first experience with guidance of atrial fibrillation ablations. *J Cardiovasc Electrophysiol*. 2006; 17(5):467-469. PMid:16684015. http://dx.doi.org/10.1111/j.1540-8167.2006.00449.x

19. Cheng Y, Wang YS, Zheng YH and Qin Y. Two-step self-assembly of nanodisks into plate-built cylinders through oriented aggregation. *J. Phys. Chem. B*. 2005; 109(23):11548-11551. PMid:16852416. http://dx.doi.org/10.1021/jp050641m

20. Zhong LS, Hu LS, Liang HP, Cao AM, Song WG and Wan LJ. Self-assembled 3D flowerlike iron oxide nanostructures and their application in water treatment. *Adv Mater*. 2006; 18(18):2426-2431. http://dx.doi.org/10.1002/adma.200600504

21. Wei XW, Zhou XM, Wu KL and Chen Y. 3-D flower-like NiCo alloy nano/microstructures grown by a surfactant-assisted solvothermal process. *CrystEngComm*. 2011; 13(5):1328-1332. http://dx.doi.org/10.1039/c0ce00468e

22. Wang H, Guo HH, Dai YY, Geng DY, Han Z, Li D et al. Optimal electromagnetic-wave absorption by enhanced dipole polarization in Ni/C nanocapsules. *Appl Phys Lett*. 2012; 101:083116. http://dx.doi.org/10.1063/1.4747811

23. Liu XG, Geng DY, Meng H, Shang PJ and Zhang ZD. Microwave-absorption properties of ZnO-coated iron nanocapsules. *Appl Phys Lett*. 2008; 92:173117. http://dx.doi.org/10.1063/1.2919098

24. Liu XG, Sun YP, Feng C, Jin CG and Li WH. Synthesis, magnetic and electromagnetic properties of Al2O3/Fe oxides composite-coated polyhedral Fe core-shell nanoparticles. *Appl Surf Sci*. 2013; 280:132-137. http://dx.doi.org/10.1016/j.apsusc.2013.04.109

25. Liu XG, Li B, Geng DY, Cui WB, Yang F, Xie ZG et al. (Fe, Ni)/C nanocapsules for electromagnetic-wave-absorber in the whole Ku-band. *Carbon*. 2009; 47(2):470-474. http://dx.doi.org/10.1016/j.carbon.2008.10.028

26. Liu XG, Geng DY, Ma S, Meng H, Tong M, Kang DJ et al. Electromagnetic-wave absorption properties of FeCo nanocapsules and coral-like aggregated self-assembled by the nanocapsules. *J Appl Phys*. 2008; 104:064319. http://dx.doi.org/10.1063/1.2982411